A Novel Numerical Technique to Enhance the Spatial Resolution of Electrical Impedance Tomography Systems

Venkatratnam Chitturi

School of Engineering, Asia Pacific University, Kualalumpur, Malaysia. chitturi@apu.edu.my

Farrukh Hafiz Nagi

Department of Mechanical Engineering, Universiti Tenaga Nasional, Selangor, Malaysia. Farrukh@uniten.edu.my

Abstract

Electrical impedance tomography (EIT) has shown significant results as a functional imaging tool. However, it is not yet fully suitable for anatomical imaging because of its poor spatial resolution. In this study, the anatomical information of the test object is obtained in the form of the boundary potentials using an EIT system. Then, the electrical conductivity/permittivity distribution within the test object is approached by the Laplacian difference equations and later solved by Liebmann's method. Valid results are visible with an underlying assumption of the electrical potential at the center of the test object. This novel technique provides more accurate readings and also converges to a stable solution faster. Accuracy from 99.555% to 99.785% is obtained within six iterations as compared to the traditional technique where the accuracy range from 99.265% to 99.630% with eight iterations for $\varepsilon_a \le 1\%$. This is first step towards better spatial resolution for the EIT systems.

Keywords: Electrical impedance tomography, Spatial resolution, Elliptic partial differential equations, Finite difference equation, Dirichlet boundary condition.

Introduction

Electrical impedance tomography (EIT) is a promising medical imaging technique. It comes with the advantages of safety, simplicity, economic efficiency and noninvasiveness as compared with the existing imaging techniques such as computed tomography (CT), magnetic resonance imaging (MRI) and X-rays. So far, EIT has shown significant results as a functional imaging tool such as in continuous monitoring of cardiac functioning, lung functioning etc. However, it is not fully suitable for anatomical imaging because of its poor spatial resolution [1]. Hardware developments including the electrode belts [2-3], current sources [4] and excitation methods along with the voltage measurement techniques [5] is visible to some extent to enhance the spatial resolution. Simultaneously, several improvements in the reconstruction algorithms can be found in the literature [6-12] to improve the spatial resolution of the EIT images.

In this work, a novel approach of numerical analysis is suggested towards better spatial resolution of the EIT systems and hence would be suitable for anatomical studies. Elliptic partial differential equations (PDE) are typically used to characterize steady state, boundary value problems and with two spatial dimensions. These can be employed to determine

the steady state distribution of an electric field in EIT applications. The distribution of an electric potential within a volume conductor through which a steady current flow is given by the solution of Poisson's equation, which reduces to Laplace's equation [13]. The Poisson's equation for the electrostatic fields can be represented in two-dimensions \boldsymbol{x} and \boldsymbol{y} as in equation (1).

$$\frac{\partial^2 V}{\partial x^2} + \frac{\partial^2 V}{\partial y^2} = \frac{\rho}{\varepsilon} \tag{1}$$

where, V is the electrostatic potential, ρ is the volumetric charge density and ε is the permittivity of the material.

For the regions containing no free charge, $\rho = 0$ and hence equation (1) reduces to a Laplace equation (equation (2)).

$$\frac{\partial^2 V}{\partial x^2} + \frac{\partial^2 V}{\partial y^2} = 0 \tag{2}$$

Equation (2) is a second order linear elliptic partial differential equation (PDE) with two independent variables (x, y) and one dependent variable, V.

The numerical solution of the elliptic PDEs is based on treating the object as a grid of discrete points or nodes and transforming the PDE into an algebraic finite difference equations as shown in figure 1, where i = 0 to m+1; m = 0,1,2,... and j = 0 to n+1; n = 0,1,2,... [14].

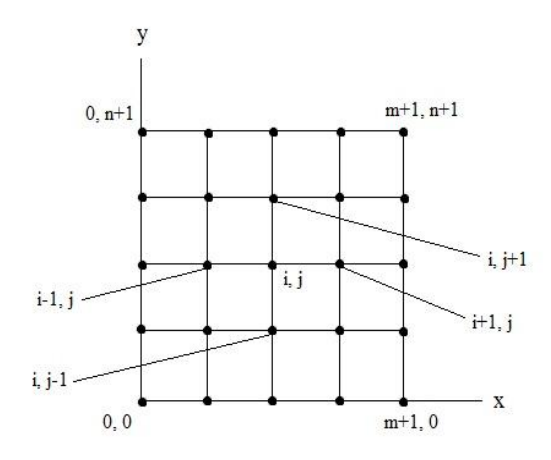


Fig 1. Grids used for the finite difference solution of elliptic PDEs with two independent variables x and v.

i. Numerical approach

The central differences based on the grid scheme (figure 1) with $\Delta x = \Delta y$ yields an equation (3).

$$V_{i+1,j} + V_{i-1,j} + V_{i,j+1} + V_{i,j+1} - 4V_{i,j} = 0$$
(3)

Equation (3) holds good for all the interior nodes and is referred to as the Laplacian difference equation. The boundary conditions must be specified in order to obtain a unique solution. The simplest case is where the voltages at the boundary is set at a fixed value. This is called a Dirichlet boundary condition. There would be more linear algebraic equations depending on the number of interior nodes. However, there are maximum five (5) unknown terms for each line (equation). For a larger sized grids, this means that a significant number of terms will be zero. This could lead to wastage of computer memory in storing zero's when full matrix elimination methods are used. Hence approximate methods are used for obtaining solutions for elliptical equations.

ii. Numerical solution

The most commonly used method is Gauss-Siedal method which when applied to partial differential equations is referred to as Liebmann's method. In this method, equation (3) is rewritten as shown in equation (4).

$$V_{i,j} = \frac{V(i+1,j) + V(i-1,j) + V(i,j+1) + V(i,j-1)}{4}$$
(4)

Equation (4) can be solved iteratively for j=1 to n and i=1 to m. Because the matrix is diagonally dominant, this procedure will converge on a stable solution. The iterations are repeated until the absolute values of all the percentage relative errors (ϵ_a)_{i,j} fall below a specified stopping criteria ϵ_s (usually 1%). These percentage relative errors are estimated by equation (5).

$$| (\varepsilon_{a})_{i,j}| = | \frac{Vi,j (new) - Vi,j (old)}{Vi,j (new)} | \times 100\%$$
 (5)

Assuming $V_{i,j}$'s as initially Zero, all ϵ_a 's for the first iteration will be 100%. The iterations are continued until this error is less than 1% [14].

Proposed System

An EIT system visualizes the distribution of electrical conductivity/permittivity within a human body. The numerical methods discussed in the above section can be applied to EIT systems for anatomical studies and hence would possibly improve/increase the spatial resolution of the EIT images. This is done by measuring the anatomical information through the boundary voltages from the electrodes and further interpolating the voltages inside the test object using the numerical methods discussed under the introduction section. Under these conditions, the parameters of the anatomical details can be further determined by beamforming techniques [15]. (next stage of this research work)

In general, consider an EIT test object with a circular boundary as shown in figure 2. Let the conductivity of the test object inside be uniform. The Laplace equation (equation (2)) for electrostatic fields can be extended in the polar coordinates \boldsymbol{r} and $\boldsymbol{\theta}$ as in equation (6).

$$\frac{\partial^2 V}{\partial r^2} + \frac{\partial^2 V}{\partial r^2} = 0 \tag{6}$$

where, r is the radius of the test object in cm and θ is the angle between the electrodes in radians.

Once again equation (6) is a second order linear elliptic partial differential equation (PDE) with two independent variables (r, θ) and one dependent variable, V.

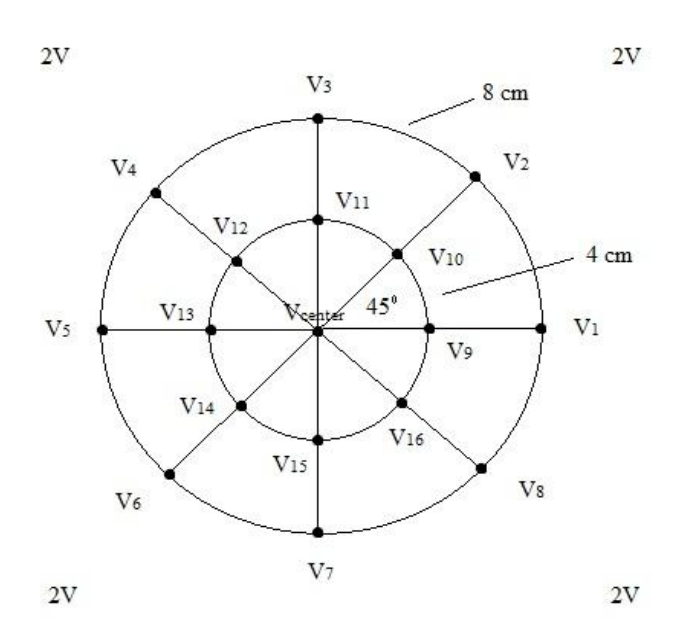


Fig 2: A circular object where the boundary voltages are held at constant voltage of 2V with uniform conductivity inside.

i. Numerical example

Let the surface diameter of the test object be 8 cm. Imagine the test object to be divided into 8 equal segments V_1 through V_8 at an angle of 45 degrees each. Let a uniform boundary voltage of 2V exist around the test object. Now consider an inner circle of diameter 4 cm with the interior nodal voltages from V_9 through V_{16} w.r.t. V_1 . The arc length for the outer radius is 3.14 cm and that of the inner radius is 1.57 cm.

Let V_{center} be the voltage at the center of the circle and is assumed as the average of the existing boundary voltages, 2V. The Laplacian difference equation for node (V_9) follows as equation (7).

$$\frac{v_9 - v_1}{2} + \frac{v_9 - v_{center}}{2} + \frac{v_9 - v_{16}}{1.57} + \frac{v_9 - v_{10}}{1.57} = 0 \tag{7}$$

where,
$$V_1 = V_{center} = 2V$$

Simplifying equation (7),

$$V_9 - 0.280 \times V_{16} - 0.280 \times V_{10} = 0.880$$
 (8)

Equations similar to equation (8) for the remaining interior nodes result in nine simultaneous equations with eight unknowns as V_{center} is known (assumed as the average of the boundary voltages, 2V, for any other value(s) of V_{center} , the electrostatic potential distribution would be misleading). This is represented in the matrix form as,

Liebmann's method is used as a solution iteratively for j=1 to n and i=1 to m. Once again the matrix is diagonally dominant and therefore converges on a stable solution. The iterations are repeated until the absolute values of all the percentage relative errors $(\epsilon_a)_{i,j}$ fall below a specified stopping criteria ϵ_s (usually 1%). These percentage relative errors are estimated by equation (5). Starting with an assumption of $V_{i,j}$'s as zero, the iterations are performed and continued until the error is less than 1% as shown in table 1.

Table 1: The interior nodal voltage values, V_9 through V_{16} after every iterations when subjected to a uniform boundary voltage of 2V. The inside of the test object is assumed to have a uniform conductivity. The stopping criteria is when all the percentage relative errors, $\epsilon_a \leq 1\%$.

Interior	Number of iterations (n)					
nodal	n = 1	n = 2	n = 3	n = 4	n = 5	n = 6
voltages						
(V)						
V_9	0.8795	1.6055	1.8556	1.9456	1.9787	1.9911
V_{10}	1.1257	1.6635	1.8709	1.9498	1.9799	1.9915
V ₁₁	1.1947	1.6851	1.8772	1.9517	1.9805	1.9921
V_{12}	1.2140	1.6927	1.8797	1.9524	1.9822	1.9930
V_{13}	1.2194	1.6952	1.8806	1.9582	1.9849	1.9939
V_{14}	1.2209	1.6960	1.9002	1.9659	1.9874	1.9947
V_{15}	1.2213	1.7652	1.9219	1.9722	1.9892	1.9953
V ₁₆	1.4676	1.8232	1.9371	1.9764	1.9905	1.9957
ε _{a max}	100%	45%	13%	4.6%	1.6%	0.62%

ii. Numerical analysis of the results

The results obtained are more accurate compared to the traditional block approach as shown in figure 1. The least accurate iterated value is 1.9911 with the most accurate iterated value of 1.9957 after six iterations. While the traditional block approach method gives a value of 1.9853 as the least accurate value to the most accurate value of 1.9963 with eight iterations. Hence the proposed method not only yields better results but also converges faster as shown in table 2.

Table 2: The interior nodal voltage values, V_9 through V_{16} calculated assuming a uniform boundary voltage of 2V, for percentage relative errors, $\epsilon_a \leq 1\%$. The inside of the test object is assumed to have a uniform conductivity.

Interior	Total number of iterations (N)			
Nodal	N = 6	N = 8		
Voltages (V)	NEW Approach	Traditional Approach		
V_9	1.9911	1.9853		
V ₁₀	1.9915	1.9852		
V ₁₁	1.9921	1.9926		
V ₁₂	1.9930	1.9852		
V ₁₃	1.9939	1.9852		
V_{14}	1.9947	1.9926		
V ₁₅	1.9953	1.9926		
V ₁₆	1.9957	1.9926		
V_{center}	2 (assumed)	1.9963 (measured)		
ε _{a max}	0.62%	0.70%		

Further accurate results can be obtained by choosing ε_a less than 1%. The rate of convergence can also be accelerated using over relaxation methods [14]

Conclusion

Elliptic partial differential equations are used to characterize steady state, boundary value problems and with two spatial dimensions to improve the spatial resolution of the EIT systems. A circular test object with a uniform boundary potential is considered. The steady state distribution of this electrical potential is found by the Laplacian difference equation in the polar form with an assumption that the central electrical potential is equal to the average of the boundary potentials. The proof of concept is shown through a working example considering a uniform boundary voltage of 2V. The inside of the test object is assumed to have a uniform conductivity. The obtained results provide more accurate readings with faster convergence rate when compared with the traditional block approach method. Hence the proposed numerical technique is suitable for spatial studies in EIT applications. The next step is to apply beamforming techniques to validate the suitability of the proposed technique for anatomical imaging.

References

- [1]. Aleksanyan et al., "Modern Trends in Development of Electrical Impedance Tomography in Medicine" Biosciences Biotechnology Research Asia, Vol. 11(Spl. Edn. 1), pp. 85-91, 2014.
- [2]. Tong In Oh et.al, "Flexible electrode belt for EIT using nanofiber web dry electrodes" Physiol. Meas. 33, IOP publishing, pp. 1603-1616, 2012.
- [3]. Matthew S. Campisi et.al, "Breast Cancer Detection Using High-Density Flexible Electrode Arrays and Electrical Impedance Tomography" IEEE, 2014.
- [4]. M Rafiei-Naeini and H McCann, "Low-noise current excitation sub-system for medical EIT" Physiol. Meas. 29, IOP Publishing, pp. S173-S184, 2008.
- [5]. Renee K. Y. Chin and Trevor A. York, "Improving Spatial Resolution for EIT Reconstructed Images through Measurement Strategies" IEEE International Conference on Signal and Image Processing Applications, 2013.
- [6]. Xiao-Ju Zhang et.al, "Modeling and simulation of open electrical impedance tomography" International Journal of Applied Electromagnetics and Mechanics 33, IOS Press, pp. 713-720, 2010.
- [7]. Kirill Y Aristovich et.al, "A method for reconstructing tomographic images of evoked neural activity with electrical impedance tomography using intracranial planar arrays" Physiol. Meas. 35, IOP Publishing, pp. 1095-1109, 2014.
- [8]. J.L. Davidson et.al, "Fusion of images obtained from EIT and MRI" Electronics Letters, Volume 48, No 11, Institution of Engineering & Technology, 2012.
- [9]. X.Y. Chen et.al, "Lung Ventilation Reconstruction by Electrical Impedance Tomography Based on Physical Information" Third International Conference on Measuring Technology and Mechatronics Automation, 2011.
- [10]. Qi Wang et.al, "Reconstruction of electrical impedance tomography (EIT) images based on the expectation maximum (EM) method" ISA Transactions 51, pp. 808-820, 2012.
- [11]. Cong Xu et.al, "Dual-modality Data Acquisition System based on CPCI Industrial Computer" IEEE, 2012.
- [12]. Ashkan Javaherian et.al, "Reducing negative effects of quadratic norm regularization on image reconstruction in electrical impedance tomography" Applied Mathematical Modelling, Volume 37, Issue 8, Pages 5637-5652, 2013.
- [13]. John S Lioumbas et.al, "Spatial considerations on electrical resistance tomography measurements" Meas. Sci. Technol. 25, doi:10.1088/0957-0233/25/5/055303, IOP Publishing, 2014.
- [14]. Steven C. Chapra and Raymond P. Canale "Numerical Methods for Engineers" 7th edition, McGraw-Hill Publication, 2014.
- [15]. Barry D. Van Veen and Kevin M. Buckley, "Beamforming: a versatile approach to spatial filtering" IEEE ASSP Magazine, 1988.